Preprint
UCRL-JC-137618

Turbulence Simulations of X-point Physics on the L-H Transitions

X.Q. Xu, R.H. Cohen, W.M. Nevins, G.D. Porter, M.E. Rensink, T.D. Rognlien, J.R. Myra, D.A. D'Ippolito, R. Moyer, P.B. Snyder, T.N. Carlstrom

This article was submitted to
18th International Atomic Energy Agency Fusion Energy Conference,
Sorrento, Italy, October 4 – 10, 2000

September 28, 2000

U.S. Department of Energy
Lawrence Livermore National Laboratory

Approved for public release; further dissemination unlimited

DISCLAIMER

This document was prepared as an account of work sponsored by an agency of the United States Government. Neither the United States Government nor the University of California nor any of their employees, makes any warranty, express or implied, or assumes any legal liability or responsibility for the accuracy, completeness, or usefulness of any information, apparatus, product, or process disclosed, or represents that its use would not infringe privately owned rights. Reference herein to any specific commercial product, process, or service by trade name, trademark, manufacturer, or otherwise, does not necessarily constitute or imply its endorsement, recommendation, or favoring by the United States Government or the University of California. The views and opinions of authors expressed herein do not necessarily state or reflect those of the United States Government or the University of California, and shall not be used for advertising or product endorsement purposes.

This is a preprint of a paper intended for publication in a journal or proceedings. Since changes may be made before publication, this preprint is made available with the understanding that it will not be cited or reproduced without the permission of the author.

This report has been reproduced
directly from the best available copy.

Available to DOE and DOE contractors from the
Office of Scientific and Technical Information
P.O. Box 62, Oak Ridge, TN 37831
Prices available from (423) 576-8401
http://apollo.osti.gov/bridge/

Available to the public from the
National Technical Information Service
U.S. Department of Commerce
5285 Port Royal Rd.,
Springfield, VA 22161
http://www.ntis.gov/

OR

Lawrence Livermore National Laboratory
Technical Information Department's Digital Library
http://www.llnl.gov/tid/Library.html

TURBULENCE SIMULATIONS OF X-POINT PHYSICS ON THE L-H TRANSITIONS[1]

X. Q. XU,[1], R. H. COHEN[1], W. M. NEVINS[1], G. D. PORTER[1], M. E. RENSINK[1], T. D. ROGNLIEN[1], J. R. MYRA[2], D. A. D'IPPOLITO[2], R. MOYER[3], P. B. SNYDER[4], T. N. CARLSTROM[4]

1) Lawrence Livermore National Laboratory Livermore, CA 94551, USA
2) Lodestar Research Corporation, Boulder, CO 80301 USA
3) University of California, San Diego, La Jolla, CA 92093 USA
4) General Atomics, San Diego, CA 92186 USA

e-mail contact of main author: xxu@llnl.gov

Abstract. We show that the resistive X-point mode is dominant mode in boundary plasmas in X-point divertor geometry. The poloidal fluctuation phase velocity from the resistive X-point turbulence shows experimentally measured structure across separatrix. The fluctuation phase velocity is larger than $E \times B$ velocity both in L and H mode phases, by at least a factor of two. We also demonstrate that there is a strong poloidal asymmetry of particle flux in the proximity of the separatrix. Turbulence suppression in the L-H transition results when sources of energy and particles drive sufficient gradients as experiemnts.

1. INTRODUCTION

The performance of tokamaks and other toroidal magnetic devices depends crucially on the dynamics of the boundary region, that is the transition region from the hot core plasma through the separatrix to the material surface of the first wall. Plasma turbulence, and the resulting anomalous cross-field plasma transport, are crucial physics processes in the boundary region, affecting on both core plasma confinement and plasma-wall interactions. Reduction of anomalous plasma transport at the boundary, associated with the transition to the H-mode operating regime, leads to sharp pedestal-like structures in the temperature and density profiles. The ubiquity of the L-H transition indicates some robust, 'universal' ingredient, such as $\boldsymbol{E} \times \boldsymbol{B}$ shear suppression which has been invoked for both internal and the H-mode transport barriers [1]. The fact that changes seem to be participated at the outer midplane is suggestive of mechanisms based on the stabilization of the ballooning modes or suppression of turbulent transport by radial electric field shear [2].

Although the H-mode can be realized in a wide variety of toroidal systems, it is most clearly associated with divertor tokamaks possessing a separatrix. It has been observed in DIII-D [3] and JET that the number of X-points and their locations in divertor configurations play an important role in determination of the H-mode power threshold. This threshold is higher in double-null (DN) divertors than in single-null (SN) divertors and is lower for forward B_t (i.e., the direction of the ion ∇B drift towards the X-point) than for reverse B_t in SN divertors [4]. It has been argued that the power threshold is not due to intrinsic plasma parameters within the separatrix, but rather parameters at the plasma

[1]Work performed under the auspices of the U. S. Department of Energy by University of California Lawrence Livermore National Laboratory under contract W-7405-ENG-48, DE-FG03-97ER54392 at LRC, and DE-FG03-95ER54294 at UCSD.

edge or in the scrape-off-layer (SOL) plasma which depend on the field line geometry. Our previous work provides physical understanding using BOUT (a 3D nonlocal electromagnetic turbulence code) simulations [5]. BOUT models boundary-plasma turbulence in a realistic divertor geometry using Braginskii equations [6] for plasma vorticity, density (n_i), electron and ion temperature (T_i, T_e) and parallel momentum. It has been found that X-point damping coupled with the change in boundary flow direction plays a crucial role in determination of the fluctuation levels. The BOUT simulation results predict higher fluctuation levels in reversed B_t than forward B_t in SN divertor tokamaks due to a change in boundary flow direction away from the X-point that impacts the strong damping near the divertor X-point [7]. The sensitivity is less in systems possessing up-down symmetry, such as a tokamak with a circular cross-section and symmetric DN divertor configurations. Theoretical symmetry considerations lead to a similar conclusion [8].

In addition to the complexity of the nonlinear dynamics of the turbulence (and unlike core plasmas), the fluctuation levels in edge plasmas are comparable to mean values and the time and spatial scales of turbulence can be comparable to that of the background parameters. To simulate a dynamically steady state in plasma boundary would require coupling the turbulence to the evolution of averaged profiles, including particle and energy sources and sinks. That requires carrying out the calculation over a transport time scale, typically on the order of $\sim 50ms$. Such a long calculation is difficult if not impossible with present computer capabilities for large-scale turbulence calculations like BOUT. However, the L-H transition typically takes place on a turbulent nonlinear time scale $\sim 100\mu s$ and BOUT is able to capture the transition dynamics.

The remainder of the paper is organized as follows. Section II discusses X-point effects on boundary turbulence and its characteristics. Results concerning the dynamics of the L-H transition are given in Sec. III. Finally, a summary of this paper is presented in Sec. IV.

2. Boundary turbulence with X-point geometry

The early stability and turbulence studies have indicated that the separatrix geometry together with characteristic steep gradients at the edge of H-mode discharge tend to introduce strong stabilizing effects for MHD ballooning modes when the X-point region has good curvature [9] and greatly reduce the turbulent thermal conductivity due to the electrostatic resistive ballooning modes [10]. The classical resistive ballooning modes falls into two separated classes based on the ordering of the resistive time scale [11]: (i) those driven by $\Delta_B^{'}$, the energy source from ideal region and (ii), Carreras-Diamond-type modes, driven by pressure gradients from within the non-ideal region. The class (i) mode is unstable only if very close to the ideal MHD stability ballooning boundary, $\beta \sim \beta_{ideal}$, where $\Delta_B^{'} \rightarrow \infty$. The necessary condition for class (ii) mode is that its growth rate, γ, must exceed the sound frequency, i.e., that $\gamma > c_s/qR$, with c_s being sound speed, R the major radius, q the safety factor. Since for circular geometry this constraint can be expressed as a condition on the toroidal mode number n, $n > const./q^{5/2}$, it suggests that the mode is always unstable in the H-mode pedestal of a separatrix plasma boundary where $q \rightarrow \infty$. The RX mode discussed here is the physical manifestation of the class (ii) modes in X-point geometry.

2.1 Resistive X-point modes

The recent studies of the resistive ballooning modes in the boundary plasma of diverted tokamaks have been given in the context of a collisional fluid model [7, 12, 13]. It is shown that the large magnetic shear and small poloidal field in the X-point region act to increase the wavenumber, and hence the importance of the resistivity, near the X-point. The resulting "disconnection" of the eigenmodes across the X-point profoundly influences the unstable spectrum. A new class of modes called resistive X-point (RX) modes exploits this synergism between resistivity and the X-point geometry, giving rise to robust growth rates at moderate-to-low mode numbers. Relative to an equivalent limited plasma, the diverted plasma is shown to be more unstable in the edge (inside the separatrix), and more stable in the scrape-off-layer. The radial profiles of linear mode characteristics calculated from the linear stability code BAL [13] are given in Figures (1). Since the mode number

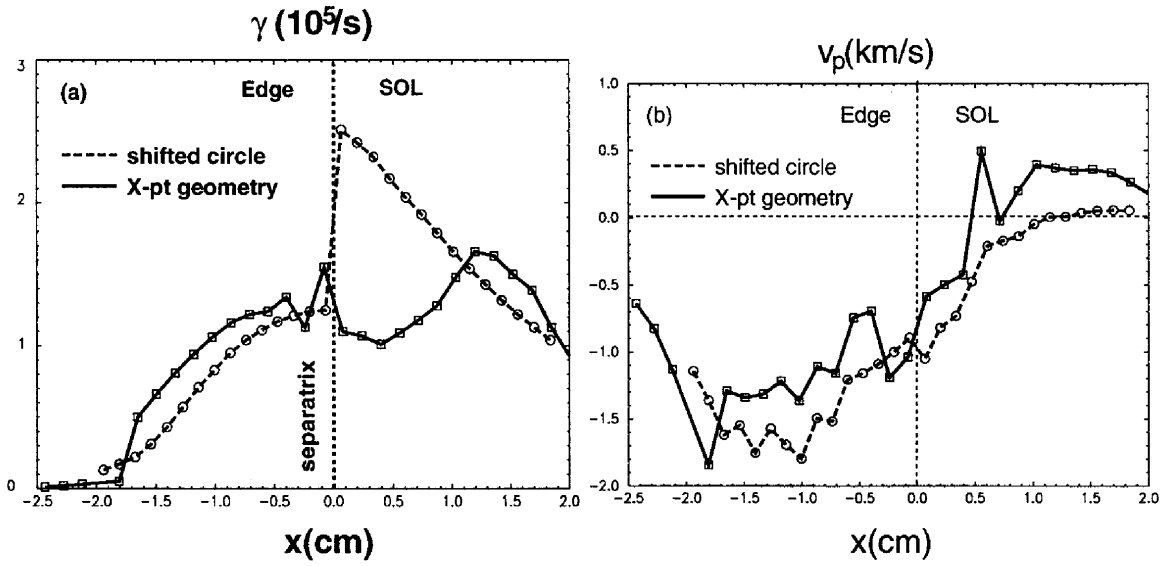

FIG. 1: (a) Linear growth rate of RX mode in X-point geometry and in shifted circle, and (b) the poloidal phase velocity in the $\boldsymbol{E} \times \boldsymbol{B}$ drift frame of RX mode in X-point geometry and in shifted circle from linear calculation

for the most unstable mode in the X-point geometry is roughly constant ($n \sim$ 40-80) in the proximity of the separatrix ($x \sim \pm 1.5cm$), the profile of the phase velocity is similar to the profile of the real frequency ($\omega = k_p v_p$ and $k_p = nB/RB_p$). The RX mode is analogous to class (ii) modes in the X-point geometry. However, the simple analytical solution of the class (ii) mode is not applicable in the boundary region across the separatrix because the two scale analysis is not valid for X-point geometry due to the very strong poloidal magnetic shear structure.

Most properties of the RX turbulence in boundary plasma are consistent with the various fluctuation measurements. From the correlation function, parameters like correlation time, poloidal correlation length and poloidal propagation velocity have been extracted from the BOUT simulations to characterize the fluctuations on DIII-D. The poloidal phase velocity v_p of the fluctuations in the midplane (Figures 2(a)) is in ion drift direction and becomes negative (electron drift direction) close to the last closed flux surface (LCFS) and into the edge of the main plasma. The velocity reversal has been observed in tokamaks, stellarators and reversed field pinch confinement devices[14]. It is also shown that the $\boldsymbol{E} \times \boldsymbol{B}$ velocity differs from the phase velocity by an amount of the order of the diamagnetic drift velocity.

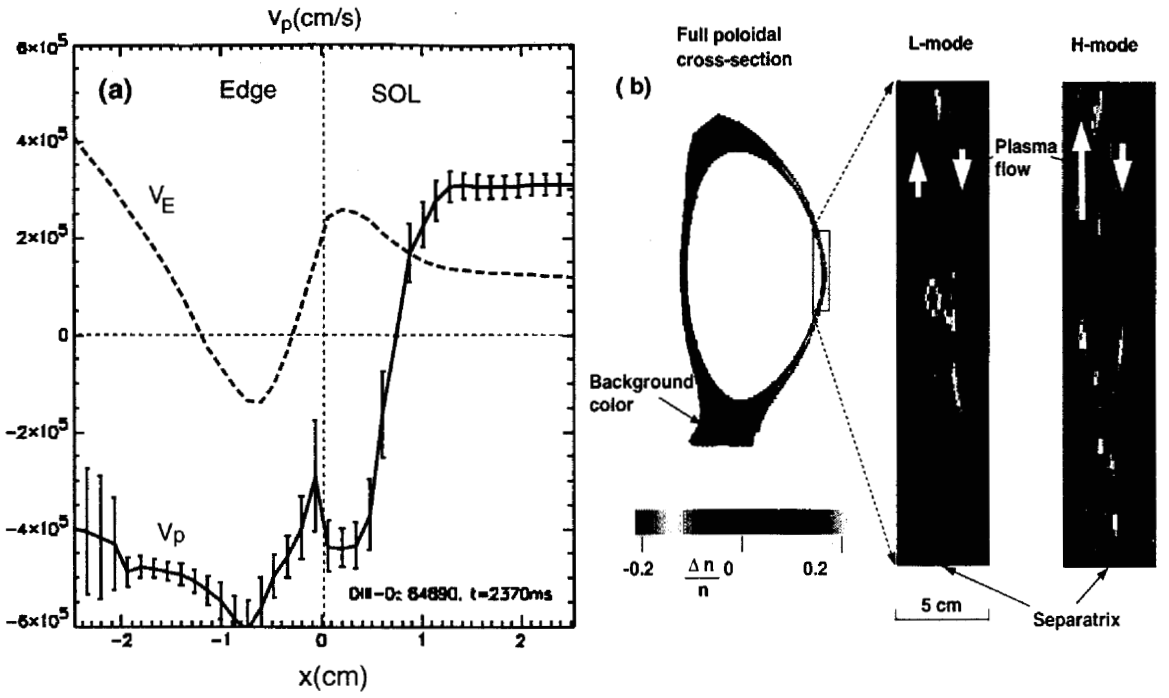

FIG. 2: (a) BOUT fluctuation phase velocity across the magnetic separatrix in boundary region and $\boldsymbol{E} \times \boldsymbol{B}$ velocity, (b) The density fluctuations at outboard mid plane. H-mode structures are broken up by flow shear.

Theory and interpretations of experimental data based the common assumption that the phase velocity is controlled by $\boldsymbol{E} \times \boldsymbol{B}$ velocity have to be modified. The reversal of the fluctuation phase velocity is due to RX turbulence, mainly inside LCFS and driven by electron skin physics coupled with bad curvature, which is in electron drift direction. Due to X-point physics, the influence of sheath physics is minimal, therefore the same RX turbulence penetrates into the SOL. Because of the electron temperature decays faster than ion temperature in the SOL, ion diamagnetic drift velocity dominates the phase velocity deeply into the SOL. According to the energy conservation, RX turbulence pumps expansion free energy from the plasma pressure gradient into flow energy via mode coupling [15, 7]. The typical fluctuation parameters obtained are a correlation time τ_c of $\sim 30\mu s$, a poloidal correlation length Δ_p of $\sim 16\rho_s$ ~ 4 cm, a radial correlation length Δ_r of $\sim 5\rho_s$ ~ 1 cm, and a poloidal propagation velocity of $\sim$500m/s in the edge and 300m/s in SOL. The radial correlation length of fluctuations is smaller than poloidal correlation length by a factor of 4, indicating oblique structures in the poloidal-radial plane. In the direction parallel to the magnetic field, the correlation length $\Delta_{||}$ is very long, $\Delta_{||} \simeq \pi q R \sim 10$m. The boundary plasma turbulence thus has a filaments structure extending only a few cm perpendicular to the magnetic field but many meters in parallel direction. These filaments are qualitatively consistent with the experimental observations from high speed movies and videos [16]. The poloidal projection of the filaments has been also called 'eddies' as shown in Fig. 2(b). For fixed background plasma profiles, there is almost no radial propagation of the turbulence. In a dynamically steady state with the sources and sinks, a very low radial (as compared to poloidal) propagation velocities of 200m/s has been found.

Particle transport perpendicular to the magnetic field Γ_r results from correlated fluctua-

tions of the plasma drift velocity $\tilde{v}_\perp$ and density $\tilde{n}$, and can be calculated from $\Gamma_r = \langle \tilde{v}_\perp \tilde{n} \rangle$. A strong poloidal asymmetry of the turbulent flux of particle is shown in Fig. 3(a). Due to

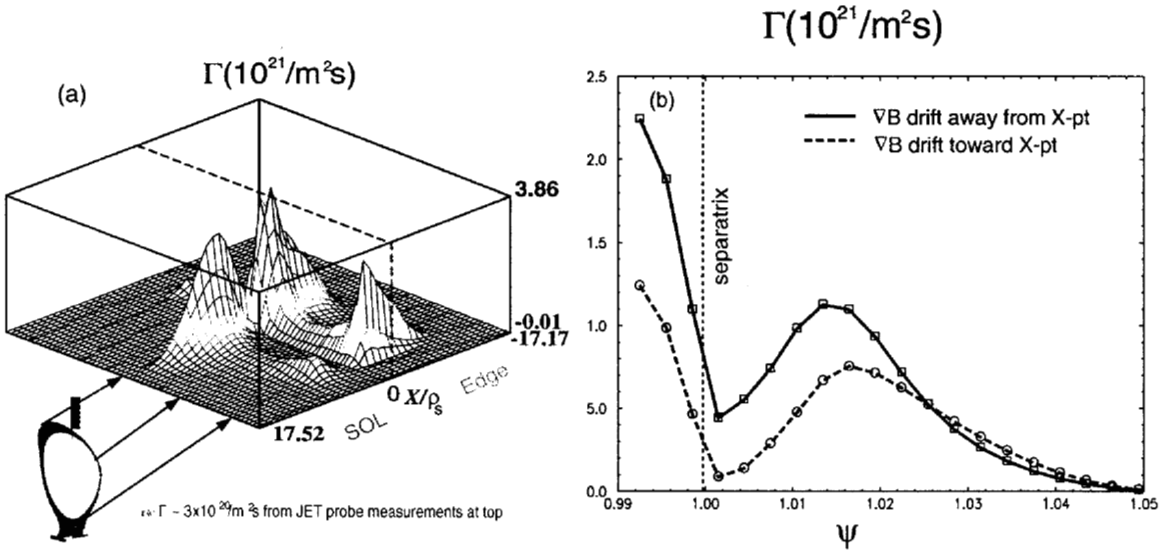

FIG. 3: The Turbulent particle flux for the ion ∇B drift towards the X-point (solid line) and ion ∇B drift away from the X-point (dashed line).

the X-point null, the plasma drift velocity $\tilde{v}_\perp \propto k_p \propto nB_t/RB_p$ diverges there as $B_p \to 0$, and thus a large particle flux is produced near the X-point region. The poloidal asymmetry of the turbulent particle flux has been reported experimentally on the limiter machines with a factor of 2 larger in low field side than high field side [17]. However, there is a much stronger poloidal asymmetry in X-point divertor geometry. This also solve the paradox from the JET probe measurements [18], where it has been reported that *the maximum of the turbulent particle flux is about a factor (3-5) larger than in limiter magnetic configuration, for similar plasma parameters, which seems to be in contradiction with the plasma global particle confinement times.* To understand the paradox, we have to understand the setup of the experiments. The turbulent particle transport has been measured in JET with a Langmuir probe array system installed on the top of the machine on the low-field side as shown in Fig. 3(a). It is then commonly assumped that the turbulent particle flux measured locally at that position is charateristic of the whole surface of the torus. For a limiter machine, an agreement within a factor of two usually was found. However, in divertor machine it can be off as much as a factor of 10 as shown in Fig. 3(a).

3.2 The effect of direction of toroidal field on the RX mode

In this section, we investigate the sensitivity of the RX mode on the direction of toroidal field B_t. This work was motivated by the discovery of the ion ∇B drift effect on the H-mode power threshold (P_{TH}), where factors of 2-3 increase in the P_{TH} are observed for the ion ∇B drift away from the X-point. In previous work the collisional transport of ions near the separatrix of a diverted tokamak plasma was shown to lead to an improvement in energy confinement [19]. The direction of the poloidally averaged collisional ion heat flux is inward if the drift is towards the X-point and outwards if the drift is away from the X-point. Thus the cross field fluxes due to the ∇B drift enter as an additional power flow across the separatrix, either adding to (ion ∇B drift toward the X-point) or subtracting from the anomalous transport to determine the threshold power for the L-H transition. This ∇B

drift effect influences the power threshold for the L-H transition, not the transition itself since it does not provide any turbulence suppression for the anomalous transport. A theoretical model of H-mode transition triggered by condensed neutrals near X-point has also been proposed [20]. Alternative to these mechanisms, the BOUT simulation results show the sensitivity of the turbulence to the direction of toroidal magnetic field B_t [7]. It has been shown that the poloidal flow V_P changes sign with the reversal of the direction of B_t by keeping everything else the same. However, the phase velocity v_p keeps the same sign, indicating $v_p > V_P$. The higher fluctuation levels in reversed B_t than forward B_t in SN divertor tokamaks was observed due to a change in boundary flow direction away from X-point that impacts the strong damping near the divertor X-point [7]. The particle transport in the case of forward is about a factor of 2 larger than the reversed B_t, as shown in Fig. 3(b).

3.3 Single-null vs. Double-null geometry

Experimental evidence suggests that the L-H transition threshold is higher in DN divertors than in SN divertors. From the power balance, the power threshold is proportional to the the anomalous transport. The higher power threshold means higher the fluctuation and transport. Therefore, we can make the comparison of turbulence properties between SN and DN configurations in the absence of the sources and sinks. To elucidate the role of the magnetic geometry, we use the same plasma profiles for both SN and DN configuration. Figures 4 shows that the RX modes are still the dominant mode in DN and fluctuation level is higher than SN by a factor of 2. The reason is that there is more averaged bad curvature drive in DN. It is worthwhile to point out that in recent experiment contrary to previous experience, the balanced DN had lower H-mode power threshold than SN. The difference would be higher trianglarity and better X-point control. The corresponding simulations is under investigation.

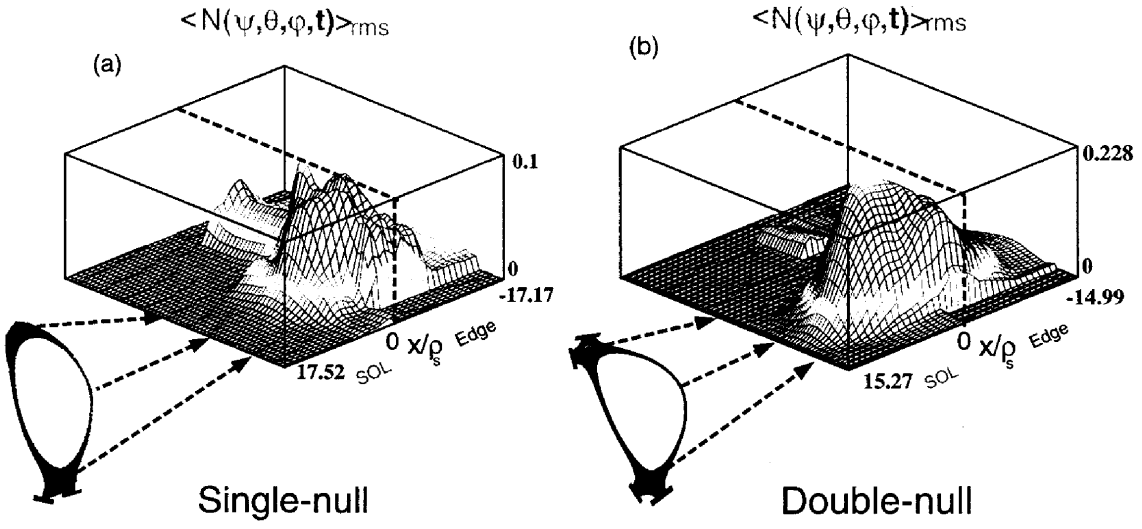

FIG. 4: (a) Ensemble averaged density fluctuation in SN X-point geometry, (b) Ensemble averaged density fluctuation in double-null X-point geometry.

The National Spherical Torus Experiment (NSTX) is a spherical torus. It has features similar to DN tokamak configurations but with different parameter regimes: large Larmor radius, thus relative thick edge pedestal and large mirror ratio. Preliminary simulation

results show that for the plasma conditions similar to DIII-D the NSTX configuration yields larger fluctuations on the high-field side of the torus inside the separatrix and shorter poloidal correlation length. The dominant modes and turbulence saturation levels, as well as transport in NSTX are similar to tokamaks such as DIII-D. These are strictly fluid studies; it is likely that there is an increased role of kinetic effects resulting from the relatively (compared to tokamaks) larger Larmor radius and smaller connection length in the spherical torus.

3. L-H transitions with sources and sinks

The L-H transition physics has been extensively studied and many theoretical models have been developed in past two decades. However, there is as yet no conclusive understanding the mechanisms of the transition [21]. Although Alcator C-mod [22] shows interesting agreement with the work in Ref. [23], comparisons with the theory and DIII-D [3, 24] and COMPASS-D [25] data show that there is no evidence for a correlation of L-H transition with a diamagnetic parameter α_{dia}. The recent H-mode plasmas have been directly produced on DIII-D by injecting frozen deuterium pellets into L-mode plasmas [24] . The pellet injected from the low toroidal field side and high field side were both able to produce H-mode transitions. The experimental results were compared with three most promised theoretical models of the H-mode [26]. It has been shown that pellet induced H-modes have L-H transitions at plasma parameters far below theoretical predictions. It is also demonstrated that by keeping toroidal field and plasma profiles the same and moving vertically to switch from lower to upper SN, the H-mode power threshold has been changed by more than a factor of two. These experiments have once again clearly shown the important role of the realistic X-point geometry in the L-H transition. Since the RX turbulence model seems to reproduce many of the features of the boundary fluctuation and transport, the properties of the L-H transition has also been explored [7]. Under DIII-D tokamak L-mode conditions, the dominant source of turbulence is curvature-driven resistive X-point modes (RX modes). With sources added in the core-edge region and sinks in the scrape-off layer (SOL), the code follows the self-consistent profile evolution together with turbulence. Results indicate that, as the power is increased, these modes are stabilized by increased turbulence-generated velocity shear, resulting in an abrupt suppression of high-n turbulence and formation of a pedestal in density and temperature, as is characteristic of the H-mode transition. In the presence of the sources, turbulence-generated velocity shear increases resulting from both higher fluctuation levels and large ion diamagnetic contribution due to steeper gradients. Owing to the three dimensional nature of the problem, a simple scaling dependence of the power threshold is not yet produced. Nevertheless, it is clearly shown that the L-H transition and the suppression of the turbulence results when sources of energy and particles drive sufficient gradients as experiments.

To demonstrate the L-H transition in the BOUT simulation, the profiles are allowed to fluctutate, and thus have to be sustained by a energy source. This source term is of the form

$$S(x) = s_0 \hat{S}(x) \tag{1}$$

$$\hat{S}(x) = exp\left(\frac{-(x - X_L)^2}{\Delta_s^2}\right) \tag{2}$$

This source term exhibits a maximum at left boundary $x = X_L$ and is such that it

decreases rapidly when approaching the separatrix. The reason for this choice is to simulate the power from the core and turbulence transport of the energy across the edge region into the SOL. The link between the source amplitude and the total input power P_{input} is given by

$$P_{input} = \frac{\sqrt{\pi}}{2} s_0 T_{i0} V \tag{3}$$

$$V = \frac{2\pi^2 R_0 a_0 \Delta_s}{N_{sim}} \tag{4}$$

where V is the source volume. In this model, the edge gradient adjusts itself such that the time average of the outflux balances the input flux (the radial integral of the source S). Figure 5(a) shows the density profile for various source amplitude. In these numerical experiments, the injected particles have the background plasma ion temperture. Thus the ion temperature remains the same with source on. This can be achieved experimentally by both pallet injection and simultaneously auxiliary heating power [24]. Clearly, the density and ion pressure profile steepens as the source amplitude increases. The time evolution of the turbulence electron heat flux $Q_{e,r} = \langle \tilde{v}_\perp \tilde{T}_e \rangle$ is illustrated in Figure 5 (b) for several source rates. It is clearly shown that for large input power, the turbulence

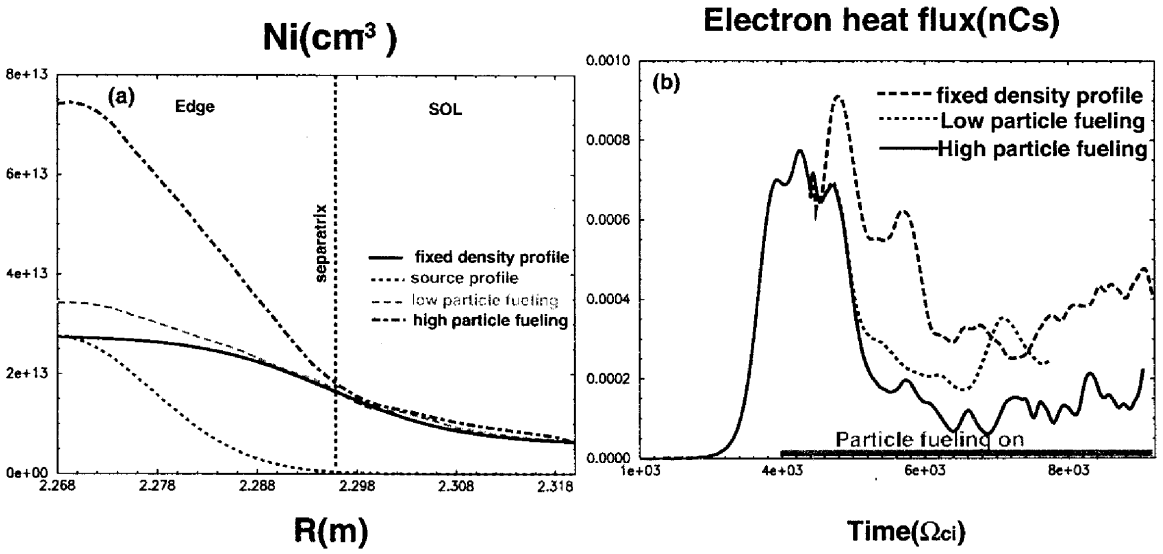

FIG. 5: (a) Plasma density profiles for the various particle fueling; (b) Time history of the electron conduction heat flux.

electron heat flux is suppressed by a factor of 4. For the case of high source amplitude with L-H transition, the corresponding $\boldsymbol{E} \times \boldsymbol{B}$ velocity and the fluctuation phase velocity is given in Figure 6(a). It is shown that both $\boldsymbol{E} \times \boldsymbol{B}$ velocity increases by a factor of 7 and the phase velocity by a factor of 2 after the transition. However, the phase velocity is still larger than the $\boldsymbol{E} \times \boldsymbol{B}$ velocity by a factor of 2. As discussed in Ref.[7], the flow shear is produced by poloidal spin-up driven by the turbulence-generated radial current near the transition. After the transition the fluctuations are quenched, and therefore the drive for the flow shear vanishes so that the ∇P_i contribution remains. Therefore the turbulent suppression remains as well. This feature is in qualitative agreement with phase-transition models [27] and the nonlinear simulations of resistive pressure gradient driven turbulence [28]. The radial profiles of the electron heat flux indicate the global

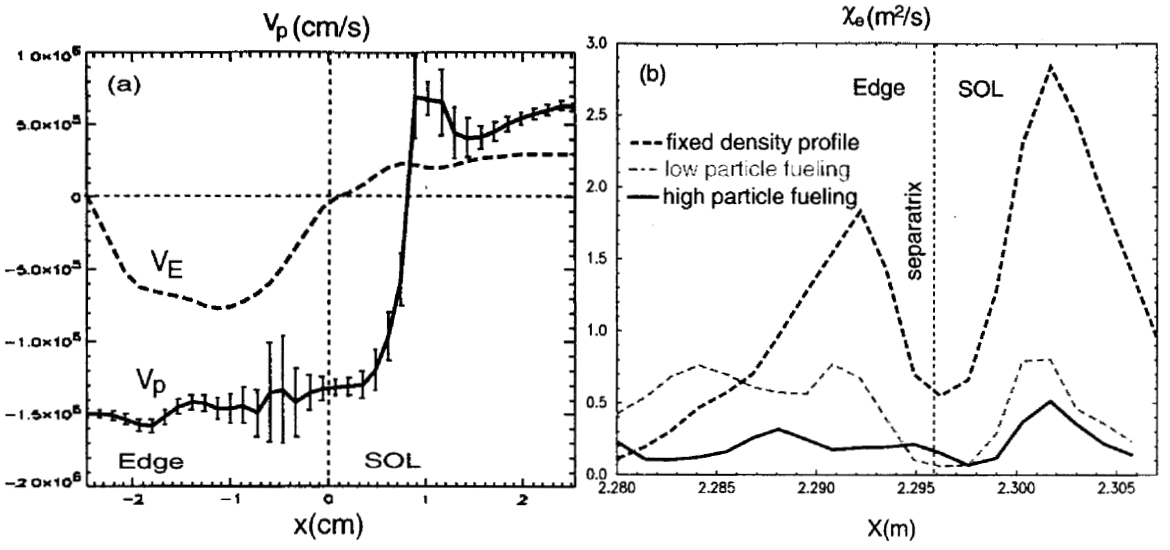

FIG. 6: (a). radial profiles of $\boldsymbol{E} \times \boldsymbol{B}$ velocity and fluctuation phase velocity across the separatrix; (b).radial profiles of electron heat diffusivity for the corresponding particle fueling.

suppression, as shown in Figure 6(b). In our previous work, we use neutral beams to heat the plasma in such a way that the ion temperature increases while the density emains constant. In this work, we ramp up the density profile while keeping the ion temperature constant. Although as a final state the plasma pressure profile is same, we find it is easy to get an L-H transition by heating ion directly because it is easy to get large negative of $E_r \sim (1/Zen)dP_i/dr$ shear.

High performance H-mode plasmas are often terminated or degraded by edge localized instabilities (ELMs). Previous studies of H-mode discharges suggest an important role for current and pressure driven modes in the intermediate range of toroidal mode numbers ($5 < n < 40$). The BOUT code has been updated to include the equilibrium bootstrap currents arising from edge pressure gradients. Including bootstrap effects, which can be especially important in Advanced Tokamak modes of operation, allows BOUT to simulate intermediate-n kink, peeling, and ballooning modes, and their interaction with RX modes. Preliminary simulations from BOUT including the Pfirsch-Schluter current show stronger linear instabilities and higher nonlinear saturation levels [29]. Results from simulations including the full equilibrium current in various parameter regimes will be given in a separate publication.

4. Summary and conclusions

BOUT contains much of the relevant physics for the pedestal barrier problem for the experimentally relevant X-point divertor geometry. Encouraging results have been obtained when using measured DIII-D profiles. The resistive X-point mode has been identified. The comparisons of the shifted-circle vs. X-point geometry show the different dominanted modes and turbulence fluctuation levels. The poloidal fluctuation phase velocity shows experimentally measured structure across separatrix. The fluctuation phase velocity is larger than $E \times B$ velocity, at least by a factor of two. A strong poloidal asymmetry of particle flux in the proximity of the separatrix helps to explain the paradox of the JET probe measurement of the particle flux. Our L-H transition with simple sources added

shows the transitions with resistive X-point modes dominating L-mode. The levels of turbulence are similar to experimental measurements. The sensitivity of L-H transition to the sign of $\mathbf{B}_t$ may be due to poloidal symmetry breaking by the poloidal flow.

5. ACKNOWLEDGMENTS

The simulations were done on the NERSC T3E and IBM SP, and on Livermore Computing/LLNL workstation clusters. We thank Drs. K. H. Burrell, P. H. Diamond, A. M. Dimits, R. J. Groebner, T. S. Hahm, S. Krasheninnikov, L. L. Lao, T. L. Rhodes, L. L. Lodestro, G. R. Mckee, L. D. Pearlstein, M. N. Rosenbluth, D. D. Ryutov, T. C. Simonen, and S. Zweben for fruitful physics discussions. We thank for Dr. A. Hindmarsh and A. Taylor on providing the PVODE PDE Solver package.

References

[1] K. H. Burrell, Physics of Plasmas Vol. **4** (1997) 1499.

[2] Moyer R A, Physics of Plasmas Vol. **2** (1995) 2397.

[3] Carlstrom, T. N., Burrell, K. H., Groebner, R. J., *et al.*, Nuclear Fusion, **39**, (1999)1941.

[4] Carlstrom, T. N., Burrell, K. H., Groebner, R. J., *et al.*, *Importance of X-point Physics on the H-mode Power Threshold in DIII-D*, GO2, 41st APS Meeting,1999; Carlstrom, T. N. Gohil, P., Watkins, J. G, *et al.*, Plasma Phys Control. Fusion 36 A147(1994).

[5] Xu, X. Q., and Cohen, R. H., Contributions to Plasma Physics, Vol. **38** 158 (1998).

[6] S. I. Braginskii, Transport processes in a plasma *Reviews of Plasma Physics*, Vol. I, Ed. M. A. Leontovich (Consultants Bureau, New York, 1965), p. 205.

[7] Xu, X. Q., Cohen, R. H., Rognlien, T. D., and Myra, J. R., Physics of Plasmas, Vol. **7**, 1951 (2000).

[8] Ryutov, D. D., and Cohen, R. H. *Symmetry Considerations in the Selection of Plasma Transport Models for Tokamaks*, UP2.12, 41st APS Meeting,1999.

[9] Bishop, C. M., Nuclear Fusion, **26**, (1986)1063.

[10] Hahm, T. S., and Diamond, P. H., Phys. Fluids Vol. **30**, (1987) 137.

[11] J. N. Connor and R. J. Hastie, Physics of Plasmas, Vol. **6**, 4260(1999).

[12] Xu, X. Q., Cohen, R. H., Porter, *et al.*, Nuclear Fusion, Vol. 40, 731 (2000).

[13] Myra, J. R., D'Ippolito, D. A., Xu, X. Q., and Cohen, R. H., Physics of Plasmas Vol. **7**, 2290 (2000).

[14] S. J. Zweben, *et. al.*, Nuclear Fusion **25** 171-183 (1985); Ch. P. Ritz, *et al.*, PRL **65** 2543 (1990); C. Hidalgo, *et al.*, Nuclear Fusion, **31**, (1991)1471; V. Antoni, *et al.*, PRL **79** 4814 (1997).

[15] Diamond, *et. al.*, PRL **84** 4842 (2000); Diamond & Rosenbluth, *et. al.*, IAEA 1998; E. Sanchez,*et. al.* , PoP **7** 1408 (2000);

[16] S. Zweben, *et al.*, 27th EPS, 2000; Endler, M., JNM 266-269 (1999)84-90.

[17] Tynan, G R 1996 Transport, Chaos and Plasma Physics 2. Equ. Turbulence Plasma (Universite de Provence, IMT Marseille, 10-22 July, 1995) (Singapore: World Scientific)

[18] I. Garcia-Cortes, *et al.*, 14th PSI-Rosenheim, 2000; I. Garcia-Cortes, *et al.*,PPCF, **42** (2000) 389-400.

[19] F. L. Hinton, Nuclear Fusion **25** 1457-1462 (1985); F. L. Hinton and G. M. Staebler, Nuclear Fusion **29** 405-414 (1989).

[20] Toda S, Itoh S-I, Yagi, M, and Miura, PPCF, **39** (1997)301-312.

[21] J. N. Connor and Wilson H R, PPCF, Vol. **42**, R1(2000).

[22] Hubbard, A E, *et al.*, PPCF, Vol. **40**, 689(1998).

[23] B. N. Rogers, and J. F. Drake, Physical Review Letters **81** (1998) 4396; B. N. Rogers, and J. F. Drake, Physics of Plasmas Vol. **6** (1999) 2797.

[24] Gohil, P., *et al.*, 2000 US-EU Transport Task Force Workshop (Burlington, USA), unpublished.

[25] Field A R, *et al.* Proc. 26th EPS Conf. 1999(P273).

[26] Rogers, R., *et al.*, 17th IAEA Fusion Energy Conf., Yokohama, Japan 1998, paper IAEA-CN-69/THP2/01; Pogutse, *et al.*, Proc. 24th EPS Conf. 1997(P3-1041); Wilson,*et al.*, 17th IAEA Fusion Energy Conf., Yokohama, Japan 1998, paper IAEA-F1-CN-69/THP3/2.

[27] Diamond P H, Liang Y-M, Carreras B A and Terry P W 1994 Phys. Rev. Lett. **72** 2565.

[28] Carreras B A, Lynch, V E, Garcia L, and Diamond P H, Physics of Plasmas Vol. **2**, 2722 (1995).

[29] Snyder, P. B., *et al.*, 27th European Physical Society Conference, 2000.